Journal of the Physical Society of Japan
Vol. 63, No. 8, August, 1994, pp. 3107–3114

Simultaneous Measurement of Thermal Diffusivity and Conductivity Applied to Bi-2223 Ceramic Superconductors

Manabu IKEBE, Hiroyuki FUJISHIRO, Tomoyuki NAITO and Koshichi NOTO

Department of Materials Science and Technology, Faculty of Engineering, Iwate University, 4-3-5 Ueda, Morioka 020

(Received March 9, 1994)

A method to measure the thermal diffusivity α and the conductivity κ under an identical experimental setup has been developed and α and κ of Bi-2223 oxide superconductor have been measured quasi-simultaneously. The results are analyzed on the basis of the BRT and Tewordt-Wölkhausen theory. The simultaneous measurement makes it possible to estimate the specific heat C and the Debye temperature Θ_D, as well as to separate the electron and phonon contributions to the diffusivity. The simultaneous measurement also provides a useful check on the reliability and the consistency of the analyses.

[thermal diffusivity, thermal conductivity, specific heat, Bi-2223 superconductor, phonon scattering, BRT and Tewordt-Wölkhausen theory]

§1. Introduction

The thermal diffusivity α of superconductive materials is an important physical parameter to discuss transient phenomena and the thermal stability of cryogenic systems. The diffusivity α is given by κ/C, the thermal conductivity κ divided by the specific heat C. In insulators, in which the heat conduction is entirely due to phonons, α is expressed as $\alpha = v^2\tau_{ph}/3$ with the phonon velocity v and the average scattering time τ_{ph}. In case of the oxide superconductors, the heat conduction is due to both phonons and charge carriers. Similarly to usual metals, the specific heat of the oxide superconductors is overwhelmingly dominated by the phonon contribution except in the extremely low temperature region. Then if we can separate out the phonon and the carrier contribution to the diffusivity of the oxide superconductors, important and direct information on the phonon scattering can be obtained. We have achieved the separation by quasi-simultaneously measuring the thermal diffusivity and the thermal conductivity.[1,2] More strictly, the diffusivity and the conductivity were successively measured at each temperature under an identical experimental setup. The results of the conductivity, the diffusivity and the estimated specific heat of the Bi-2223 sintered polycrystal are analyzed systematically and self-consistently in this study. The contributions of several phonon scattering mechanisms are determined quantitatively.

§2. Experimental Procedure

2.1 *Experimental setup*

Figure 1 shows a schematic view of the sample setup on the cold head of a Gifford-McMahon (GM) cycle helium refrigerator which was used as the cryostat.[3] The attachment of both the Bi-2223 sample to the cold-finger of the GM refrigerator and a metal film resistance heater (10 kΩ) to the sample was made by use of GE7031 varnish. AuFe(0.07 at.%)-Chromel thermocouples with diameter 73 μm were used as thermometers. The temperature range for the measurement was from 15 to 180 K. The sample was enclosed by a radiation shield of Ni-plated Cu which was thermally anchored to the cold head. The whole sample chamber was evacuated to 1×10^{-6} Torr by an oil diffusion pump. Under this experimental setup, the thermal conductivity was measured

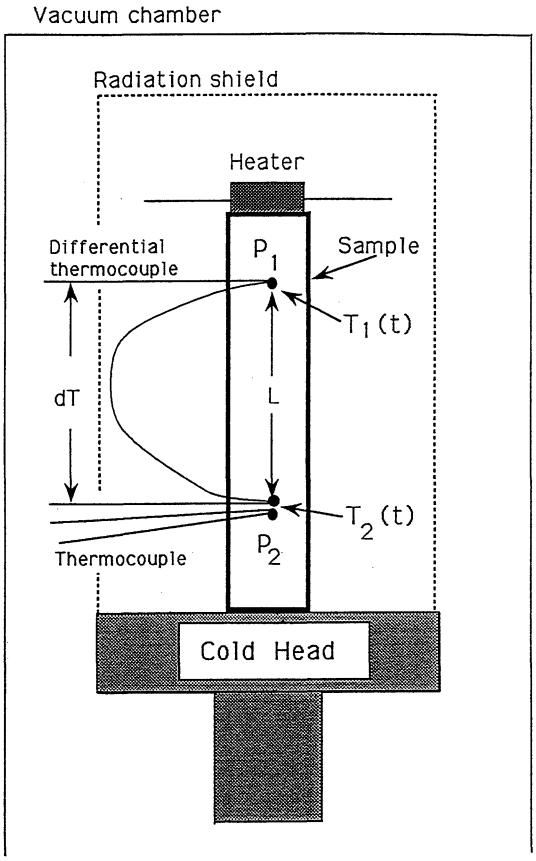

Fig. 1. Schematic diagram of the experimental set up on the cold head of the closed cycle helium refrigerator.

by a standard steady heat-flow method. The thermal diffusivity was measured by an arbitrary heating method prior to the conductivity measurement at each fixed temperature. An automatic measuring system was made by use of a personal computer (NEC 9800 series) and RS-232C and GP-IB bus lines, including the GM closed cycle helium refrigerator.[1,3] The Bi-2223 polycrystals for this study were prepared by pressing and sintering $Bi_{1.85}Pb_{0.35}Sr_{1.90}Ca_{2.05}Cu_{3.05}O_X$ powders (Dowa Mining Co. LTD.) at 840°C for 50 hours. The procedure to determine the diffusivity is explained in the following subsection.

2.2 *Determination of the diffusivity* α[1)]

When a heat pulse is transmitted from a heater into a sample of long and slender shape, the time variation of temperature $T(x, t)$ is described by the one dimensional diffusion equation,

$$\frac{\partial T(x,t)}{\partial t}=\alpha\frac{\partial^2 T(x,t)}{\partial x^2}, \tag{1}$$

where t is the time and x is the space coordinate. This equation can be numerically solved by the Crank-Nicolson implicit method.[4] The t-axis and the x-axis are divided by the respective unit of Δt and Δx to define discrete "lattice points" $u[i, j]$. Then eq. (1) is transformed to approximate difference equations given by

$$\begin{aligned}&(1+A)u[i,j+1]-A(u[i-1,j-1]+u[i+1,j+1])/2\\&\quad=(1-A)u[i,j]+A(u[i-1,j]+u[i+1,j])/2,\end{aligned} \tag{2}$$

where A is a kind of the normalized diffusivity and equal to $\alpha\Delta t/(\Delta x)^2$. By applying a boundary condition to eq. (2), eq. (1) is finally converted into n-dimensional linear equations, which can be solved by the Gauss elimination method. We calculated the temperature change $T(x, t)$ at arbitrary x and t with the time division $\Delta t=0.32$ sec and the space division $\Delta x=0.5$ mm for various values of α. The calculation was performed by a personal computer on a FORTRAN program. In the experiment, a current pulse of width $3\sim5$ seconds was applied and the $T_1(t)$ and $T_2(t)$ in Fig. 1 were recorded for 3.1 times a second in the time span of $100\sim200$ seconds. Then $T_1(t)$ at the point P_1 is used for the boundary condition to the diffusion equation for $T_2(t)$ at the point P_2. The use of the experimentally measured $T_1(t)$ as the boundary condition resolves the ambiguity due to the heat capacity of the heater and due to the various heat resistance between the heater and the sample surface.

Figure 2(a) shows an example of $T_1(t)$ and $T_2(t)$ after impression of the 7.5 mA and 3 seconds current pulse at 170 K. Figure 2(b) shows an example of a fitting of the measured $T_2(t)$ and the calculated $T_2'(t)$. For systematic determination of α values, the maximum values of

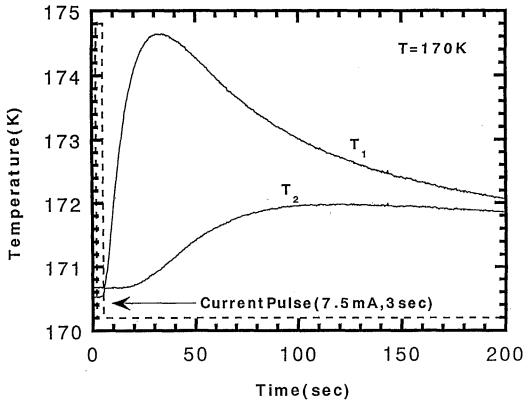

(a)

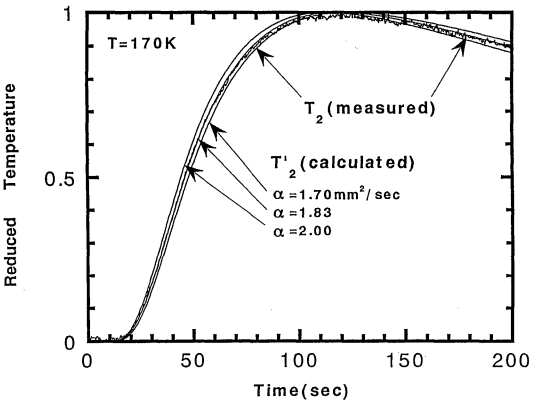

(b)

Fig. 2. The procedure for determination of the diffusivity. (a) time variations of the temperatures at two measuring points (T_1 and T_2) after applying a current pulse. (b) an example of the fitting of the measured curve (T_2) to the calculated one (T_2').

the measured and the calculated $T_2(t)$ were normalized to 1 and eighty points between 10% and 90% of the rising curve of $T_2(t)$ were sampled to give the minimum square time error $\langle \Delta t^2 \rangle$. This method of the diffusivity measurement had been confirmed to have $\pm 1.5\%$ precision and $\pm 5\%$ accuracy for a variety of specimens with various α values.

§3. Experimental Results

The electrical resistivity of a sintered Bi-2223 sample is shown in Fig. 3 as a function of the temperature T. The resistivity curve shows a sharp superconducting transition at 108 K, which suggests good homogeneity of the sample. Figure 4 shows the temperature dependence of the thermal conductivity κ between 15 K and 180 K. As the temperature decreases, the conductivity gradually decreases down to near T_c, then remarkably increases below T_c, takes the maximum around 70 K and sharply decreases with the further decrease of T. This temperature dependence agrees with the widely observed behavior of κ for the oxide superconductors.[5-8]

Figure 5 shows the temperature dependence of the thermal diffusivity α of the Bi-2223 polycrystal. Between 180 K and T_c, α increases

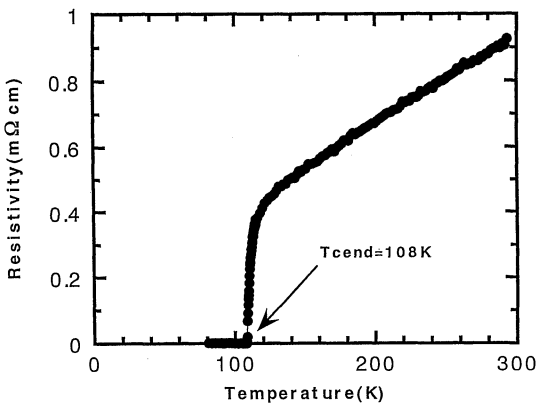

Fig. 3. The temperature dependence of the electrical resistivity of the Bi-2223 sintered sample used in this study.

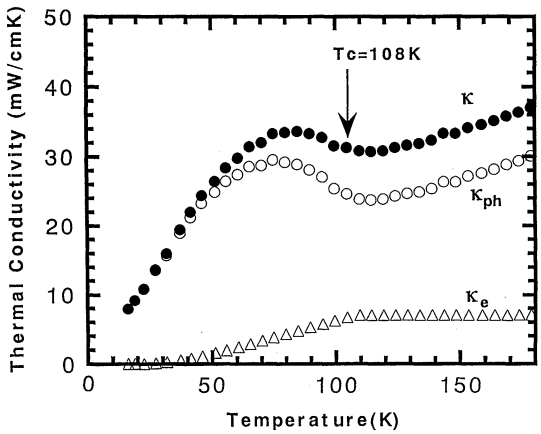

Fig. 4. The temperature dependence of the thermal conductivity κ (●). The electron contribution κ_e (△) is estimated by the WF law above T_c and Kadanoff's formula below T_c (see the text). The phonon contribution κ_{ph} (○) is given by the difference, $\kappa_{ph}=\kappa-\kappa_e$.

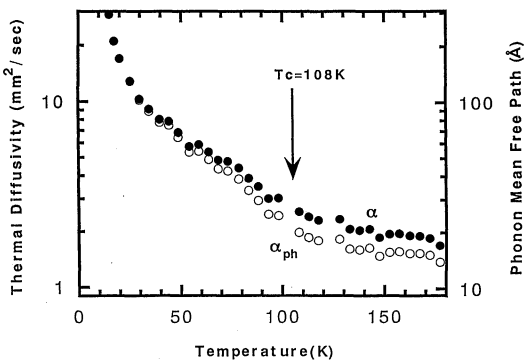

Fig. 5. Temperature dependence of the thermal diffusivity α (●). The phonon component (○) is obtained by subtracting the electron component. The electron contribution is estimated by the WF law ($T > T_c$) and Kadanoff's formula ($T < T_c$). The right hand ordinate gives the phonon mean free path l_{ph} appropriate to α_{ph}.

very gradually with decreasing temperature. The increase of α becomes remarkable around T_c and becomes very steep below about 30 K. The temperature dependence and the magnitude of α of the present observation are in rough agreement with those reported by Onuki *et al.*[9,10]

§4. Discussion

4.1 *Separation of the phonon and carrier contributions to the thermal conductivity and diffusivity*

As is well known, the thermal conductivity of metals is given by two contributions,

$$\kappa = \kappa_{ph} + \kappa_e. \tag{3}$$

Here κ_{ph} is the conductivity due to phonons and κ_e is the conductivity due to the electrons. Analogously, we define two contributions to α by the following relation,

$$\alpha = \frac{\kappa}{C} = \frac{\kappa_{ph}}{C} + \frac{\kappa_e}{C} = \alpha_{ph} + \alpha_e, \tag{4}$$

where C is the specific heat per unit volume. In simple metals, the separation of the two components of the conductivity is made by use of the Wiedemann-Franz (WF) law,

$$\frac{\kappa_{en}}{\sigma T} = \frac{\pi^2}{3e^2}, \tag{5}$$

where κ_{en} is the electronic thermal conductivity in the normal state and σ is the electrical conductivity. In ordinary metals, the WF law fails at intermediate temperatures where the electrical resistivity ρ deviates from the T linear dependence. The resistivity of oxide superconductors shows the characteristic T linear dependence over quite a wide temperature range as can be seen in Fig. 3. Accordingly, the WF law is expected to hold over the entire temperature range above T_c for the oxide superconductors and to result in constant and small κ_{en}, making a marked contrast to ordinary metals.

Below T_c, the charge carriers which have condensed in the ground state do not contribute the heat conduction and the electronic component κ_{es} is expected to decrease with lowering temperature. Among the several theories[11-13] which treat κ_{es}, we refer to Kadanoff's formulation[11] with a minor revision to adapt to the observed linear dependence of ρ,

$$\frac{\kappa_{es}}{\kappa_{en}} = \frac{3}{2\pi^2}\int_0^\infty d\varepsilon\,\varepsilon^2\,\mathrm{sech}^2\left\{\frac{1}{2}[\varepsilon^2+(\beta\Delta)^2]^{1/2}\right\}\frac{\left[1+\mathbf{a}\dfrac{T}{T_c}\right]}{\left[\dfrac{\varepsilon}{\{\varepsilon^2+(\beta\Delta)^2\}^{1/2}}+\mathbf{a}\dfrac{T}{T_c}\right]}. \tag{6}$$

Here, $\boldsymbol{a}$ represents the ratio of the T-linear electrical resistance at T_c to the residual impurity resistance, β is $1/k_B T$ and Δ is the BCS energy gap. In Fig. 4, κ_{en} estimated by eq. (5) and κ_{es} estimated by eq. (6) are also presented. The separation of the phonon and the carrier contribution to the thermal diffusivity α can readily be achieved on the basis of the corresponding separation for κ by the following equation,

$$\frac{\alpha_e}{\alpha_{ph}} = \frac{\kappa_e}{\kappa_{ph}}. \tag{7}$$

The temperature dependence of α_{ph} estimated

in this way is plotted in Fig. 5.

The kinetic theory of the thermal conductivity gives the following formula for the phonon contribution,

$$\kappa_{ph}=\frac{1}{3}C_{ph}v^2\langle\tau_{ph}\rangle, \tag{8}$$

where C_{ph} is the phonon specific heat per unit volume, v the sound velocity and $\langle\tau_{ph}\rangle$ is the averaged phonon scattering time. If the electronic contribution to the specific heat (C_e), which is quite small compared to C_{ph} except at extremely low temperatures, is neglected (i.e., $C=C_{ph}$), then α_{ph} defined by eq. (4) is given by

$$\alpha_{ph}=\frac{1}{3}v^2\langle\tau_{ph}\rangle=\frac{1}{3}vl_{ph}, \tag{9}$$

where l_{ph} is the mean free path of the phonon. The mean free path l_{ph} and $\langle\tau_{ph}\rangle$ can be directly estimated from the values of α_{ph} if we know the sound velocity v. The value of v is taken to be 2.93×10^3 m/sec according to Yusheng *et al.*[14] and the obtained l_{ph} is given by the right hand ordinate in Fig. 5.

If we adopt the κ_{es} estimation due to other theories,[12,13] slightly different temperature dependence of κ_{es} is obtained. The choice of the theories, however, is not of main importance in the discussion of the present study because κ_e itself is small in the present Bi-2223 crystal as already mentioned.

4.2 *The specific heat and the Debye temperature determined from the κ and α measurement*

From the definition of the diffusivity, eq. (4), the specific heat can be determined from the simultaneously measured values of κ and α. The obtained specific heat of the present Bi-2223 sintered crystal is presented in Fig. 6. In Fig. 6 the specific heat per mole C_M is presented, which was estimated by use of the measured density value of the sample. The magnitude of C_M in Fig. 6 is in agreement with those of direct specific heat measurements,[15,16] which supports the reliability of our κ and α measurement. Because the phonon contribution is by far dominant than the electronic contribution in the temperature range studied, the specific heat data were fitted by the following Debye formula,

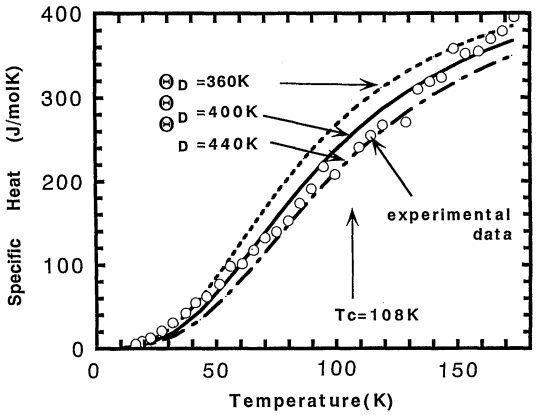

Fig. 6. The specific heat estimated from κ and α. The Debye formula with $\Theta_D=400$ K gives a pretty good overall fitting.

$$C_{Mph}=9nR\frac{T^3}{\Theta_D^3}\int_0^{\Theta_D/T}\frac{x^4e^x}{(e^x-1)^2}dx, \tag{10}$$

where x is the reduced phonon frequency, n ($=19$) the number of atoms composing Bi-2223 molecules, R the gas constant and Θ_D is the Debye temperature. Although a single Θ_D fitting fails to give a unified strict fitting over the entire temperature range, but $\Theta_D=400$ K gives a satisfactory fitting between $T=50$ to 170 K as is shown in Fig. 6. This value of Θ_D is used for the analyses of κ and α in the following subsections.

4.3 *Analyses of the thermal conductivity based on the TW-BRT theory*

Taking account of the frequency dependence of the various phonon scattering mechanism and assuming Matthiessen's rule for the scattering rate, the kinetic formula eq. (8) for the thermal conductivity was generalized by Tewordt and Wölkhausen (TW)[17] to the following equation;

$$\kappa_{ph}=\frac{3dnRT^3v^2}{M\Theta_D^3}\int_0^{\Theta_D/T}\frac{x^4e^x}{(e^x-1)^2}\tau_{ph}\,dx, \tag{11}$$

where d is the mass density, M is the mass of 1 mole of the crystal and phonon relaxation time τ_{ph} is given by

$$\frac{1}{\tau_{ph}}=\tau_b^{-1}+sT^2x^2+pT^4x^4+ETxg. \tag{12}$$

Here, τ_b is the phonon relaxation time due to

grain boundaries and s, p and E refer to the strength of the phonon scattering by sheet-like faults, point defects and charge carriers, respectively. The function $g(x, y)=\tau_{phn}/\tau_{phs}$ stands for the ratio of the phonon-electron scattering rate in the normal and superconducting state, which depends on the energy gap through the parameter $y=\Delta(T)/k_BT$. Since the charge carriers which have condensed in the ground state do not scatter phonons, $g(x, y)$ becomes smaller than 1 below T_c, which causes the observed κ_{ph} maximum in the superconducting state. The exact form of $g(x, y)$ was given by Bardeen, Rickayzen and Tewordt (BRT).[12] Experimentally obtained κ_{ph} was analyzed on the basis of eq. (11) and eq. (12). With $\Theta_D=400$ K from the specific heat and the parameter values in Table I, the theoretical curve reproduces the measured $\kappa_{ph}(T)$ quite satisfactorily as shown in Fig. 7. Figure 7 also presents the fictitious κ_{ph} curves in the absence of the phonon-carrier scattering (κ'_{ph}) and in the full presence of the phonon-carrier scattering (κ''_{ph}). These curves were also estimated by using the parameter values in Table I.

4.4 *Analyses of the phonon thermal diffusivity based on the TW-BRT theory*

In this subsection, the analyses of the phonon diffusivity are given within the framework of the Debye specific heat theory and TW-BRT analyses for the thermal conductivity in the preceding subsections. From the definition of the phonon diffusivity (eq. (4)) and neglecting the electronic contribution to the specific heat, α_{ph} is obtained by dividing eq. (10) by eq. (11), i.e.,

$$\alpha_{ph}=\frac{v^2}{3}\frac{\int_0^{\Theta_D/T}\frac{x^4e^x}{(e^x-1)^2}\tau_{ph}\,dx}{\int_0^{\Theta_D/T}\frac{x^4e^x}{(e^x-1)^2}\,dx}=\frac{v^2}{3}\langle\tau_{ph}\rangle \quad (13)$$

It should be noticed that eq. (13) does not contain additional parameters such as d, M and n in contrast to eq. (11). Thus the numerical fitting of α_{ph} to the experimental data is, in principle, more straightforward than the fitting of κ_{ph}. The results of the α_{ph} fitting based on the parameter values in Table I is shown in Fig. 8. The calculated curve reproduces the experimental data very well between 50 K and 170 K, though deviation becomes somewhat clear below 40 K. This deviation corresponds to the deviation of C_{ph} from the Debye formula in Fig. 6 and comes from the limitation of the single Θ_D analyses. However, the satisfactory agreement of the theoretical curve with the experimental observation of C_{ph}, κ_{ph} and α_{ph} between 50 K and 170 K is a strong support for the reliability of the present analyses, at least in this temperature range.

In Fig. 9, the estimated curves which indicate the contribution of each scattering mechanism to the total phonon scattering rate $1/\tau_{ph}$ are given as a function of temperature. The curves are calculated from eq. (13) by as-

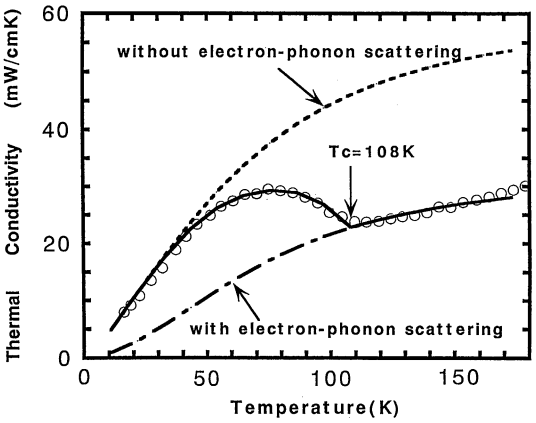

Fig. 7. The fitting of κ_{ph} by the TW-BRT theory. The solid line is the calculated curve using parameter values in Table I. The dotted line presents the estimated curve in the absence of the electron scattering. The dashed line presents the estimated curve when the electron scattering is at full work also below T_c.

Table I. Characteristic parameters of the Bi-2223 sintered superconductor.

T_c (K)	108.0
Θ_D (K)	400
M (g/mol)	1061.61
v (m/sec)	2930
d (g/cm^3)	5.334
τ_b^{-1} (sec^{-1})	1.257×10^9
p (K^{-4} sec^{-1})	92.42
s (K^{-2} sec^{-1})	1.617×10^7
E (K^{-1} sec^{-1})	2.445×10^9
λ	1.06

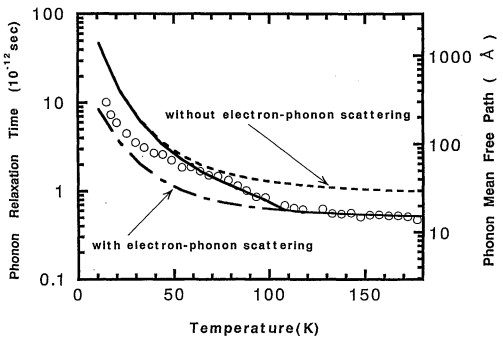

Fig. 8. The fitting of α_{ph} by the TW-BRT theory. The dashed line is the theoretical curve by use of the parameter values in Table I. The dotted line and the dash-dotted line stand for the estimated curves in the absence of and in the full presence of the electron scattering, respectively. The left hand ordinate gives the phonon relaxation time and the right hand ordinate gives the phonon mean free path.

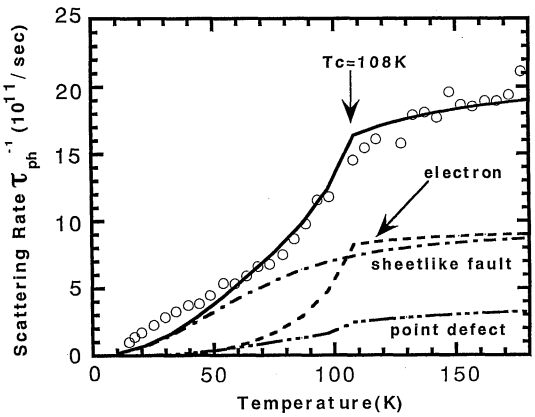

Fig. 9. The calculated scattering rate showing the contributions of various mechanism: total (——), electron (– – – –), sheet-like fault (–·–·–) and point defect (–·–·–·–·–). The estimation is based on the parameter values in Table I.

suming that a certain scattering center was removed. We find that [1] the electron scattering is dominant above T_c but sharply diminishes below T_c; [2] the sheet-like fault is an important scattering center both below and above T_c; [3] the point defect scattering contributes at higher temperatures. The boundary scattering time is estimated to be $\tau_b = 7.95 \times 10^{-10}$ sec, which corresponds to the mean free path $\lambda_b = 2.33\ \mu$m.

Finally, we make a rough estimation of the electron-phonon coupling constant λ. Tewordt and Wölkhausen[17] gave an expression of λ in terms of the electron scattering parameter E, which is given by

$$\lambda \approx \frac{2a\langle t\rangle E}{\pi v}, \tag{14}$$

where a is an average of the lattice constant and $\langle t\rangle$ is the effective hopping matrix element for a two dimensional band of electrons. If we take the values of $a = 4$ Å and $\langle t\rangle = 5000$ K following TW, then λ is estimated to be 1.06.

§5. Summary

A method to measure the thermal conductivity κ and the thermal diffusivity α under an identical experimental setup was developed and applied to the Bi-2223 polycrystal. The simultaneous measurement of κ and α made it possible to separate the phonon and electron contributions to the diffusivity and to estimate the specific heat. The Debye temperature was determined from the estimated specific heat and both the phonon thermal conductivity and diffusivity were analyzed based on the theories due to Tewordt and Wölkhausen and Bardeen, Rickayzen and Tewordt. The systematic and synthetic analyses which assume the phonon as the dominant heat carrier provided satisfactory agreement between the theory and the experimental results. The contributions of each phonon scattering mechanism were estimated and separated out as a function of temperature. The electron-phonon coupling parameter λ is estimated to be ≈ 1.1 for the sintered Bi-2223.

Acknowledgments

The authors wish to thank Dr. M. Matsukawa of Iwate University for his contribution to the computer calculation and valuable discussion.

References

1) H. Fujishiro, T. Naito, M. Ikebe and K. Noto: Cryogenic Engineering **28** (1993) 533 [in Japanese].
2) H. Fujishiro, M. Ikebe, T. Naito, M. Matsukawa and K. Noto: Cryogenic Engineering **28** (1993) 582 [in Japanese].
3) N. Hobara, M. Matsukawa, N. Matsuura, H. Fujishiro and K. Noto: Cryogenic Engineering **28**

(1993) 688 [in Japanese].
4) J. Crank: *The Mathematics of Diffusion* (Clarendon Press, London, 1975) 2nd ed., p. 144.
5) C. Uher and A. B. Kaiser: Phys. Rev. B**36** (1987) 7135.
6) J. L. Cohn, S. A. Wolf and T. A. Vanderah: Phys. Rev. B**45** (1992) 511.
7) M. F. Crommie and A. Zettl: Phys. Rev. B**41** (1990) 10978.
8) S. D. Peacor and C. Uher: Phys. Rev. B**39** (1989) 11559.
9) M. Onuki, T. Higashi, T. Fujiyoshi and K. Miyahara: *Proc. Beijing Int. Conf. High-Temp. Supercon. (BHTSC '92), Beijing, 1992*, p. 217.
10) T. Higashi, M. Onuki, S. Ishii, H. Kubota and T. Fujiyoshi: Physica C **185–189** (1991) 1257.
11) L. P. Kadanoff and P. C. Martin: Phys. Rev. **124** (1962) 670.
12) J. Bardeen, G. Rickayzen and L. Tewordt: Phys. Rev. **113** (1959) 982.
13) L. Tewordt: Phys. Rev. **129** (1963) 657.
14) H. Yusheng, X. Jiong, Z. Jincang, H. Aisheng, C. Fangao and L. Fuxue: Modern Phys. Lett. B**4** (1990) 651.
15) N. Okazaki, T. Hasegawa, K. Kishino, K. Kitazawa, A. Kishi, Y. Ikeda, M. Takano, K. Oda, H. Kitaguchi, J. Takada and Y. Miura: Phys. Rev. B**41** (1990) 4296.
16) J. E. Gordon, S. Prigge, S. J. Collocott and R. Driver: Physica C **185–189** (1991) 1351.
17) L. Tewordt and T. Wölkhausen: Solid State Commun. **70** (1989) 839.